

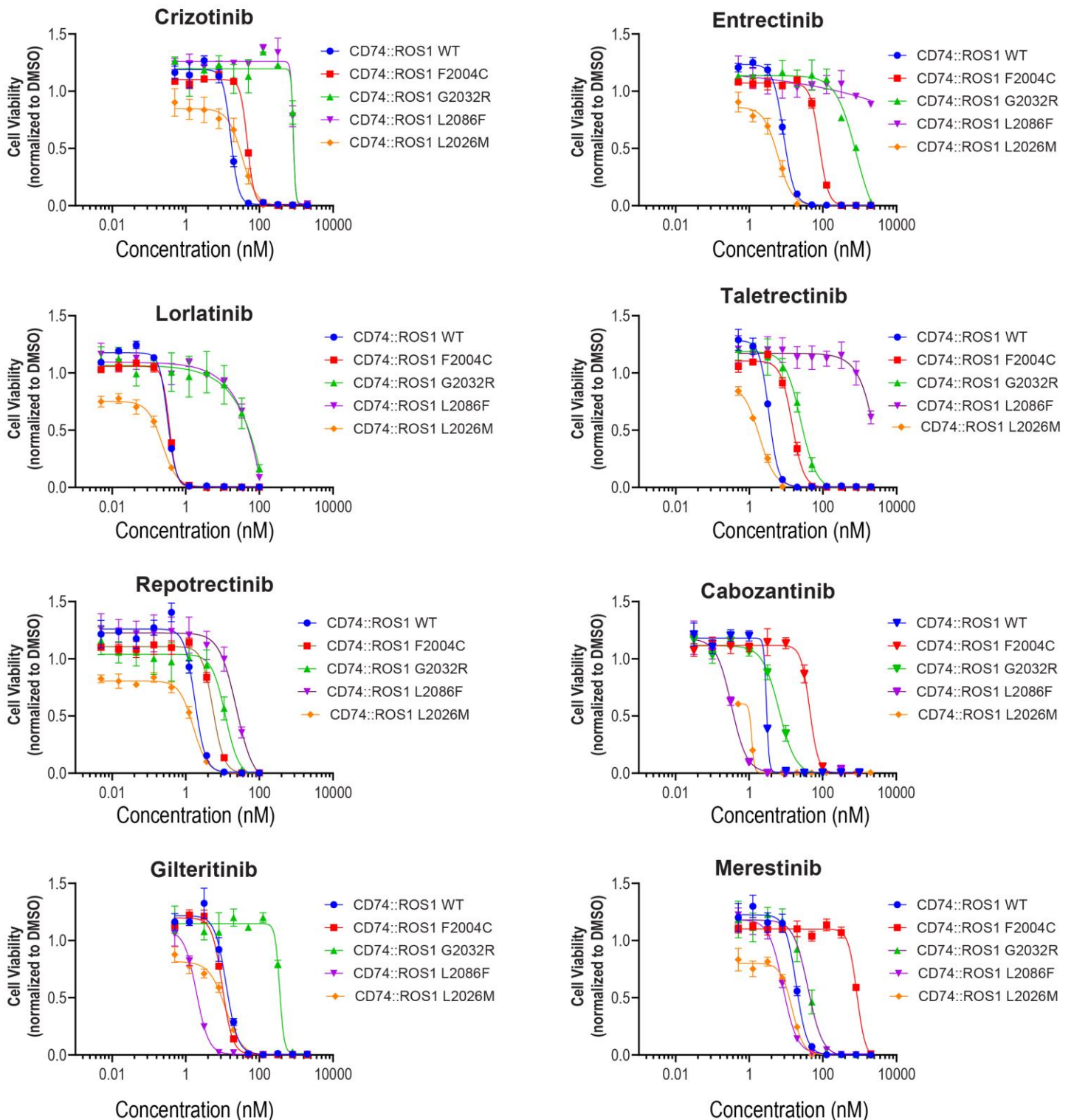
Supplementary Information

TKI Type Switching Overcomes ROS1 L2086F in ROS1 Fusion-Positive Cancers

Rajat Thawani^{1#}, Matteo Repetto^{2#}, Clare Keddy³, Katelyn Nicholson³, Kristen Jones³, Kevin Nusser³, Catherine Z. Beach³, Guilherme Harada², Alexander Drilon^{2,4*}, Monika A. Davare^{3,5*}

Supplementary Figure 1

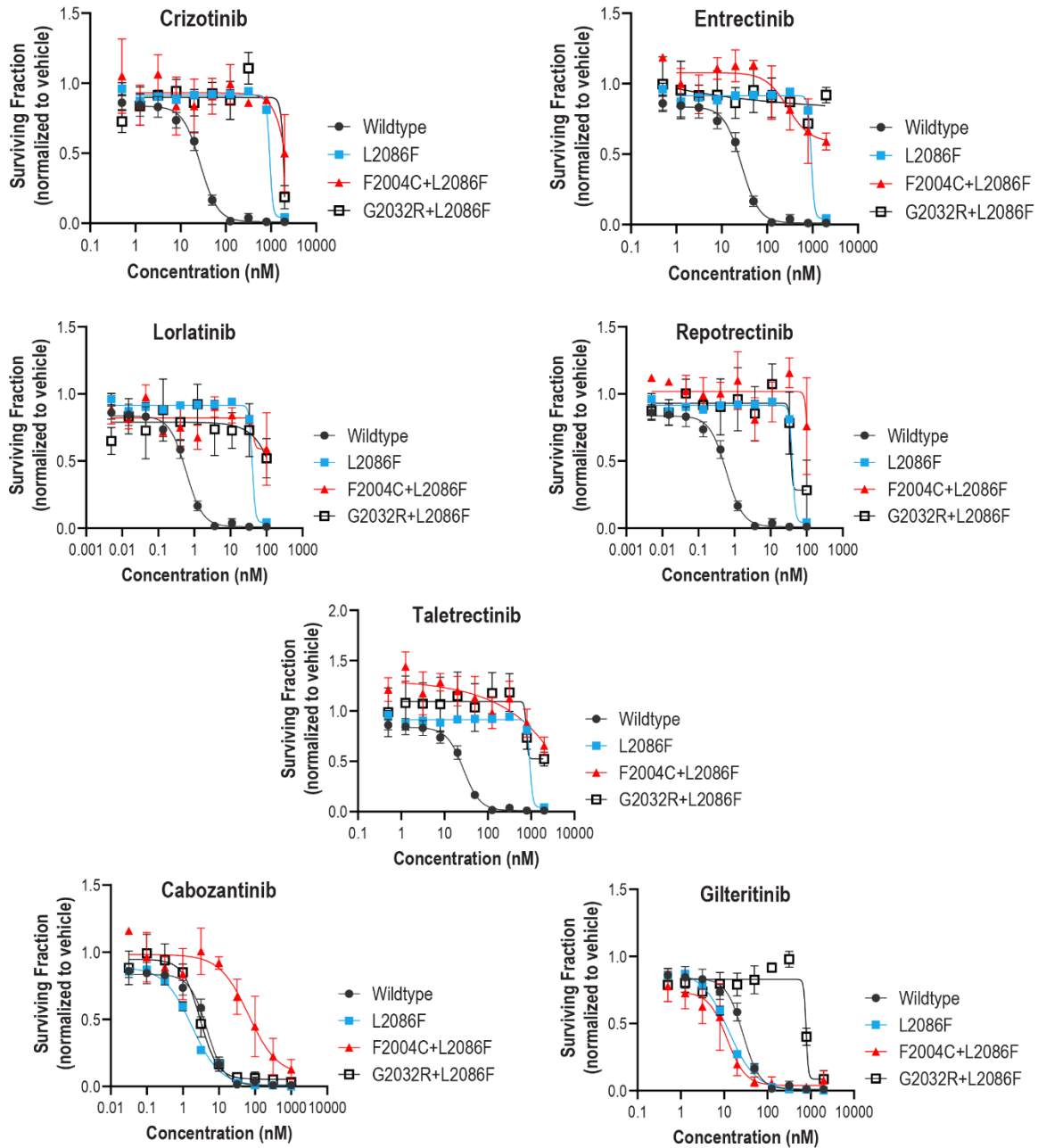
Ba/F3 CD74-ROS1



Supplementary Figure 1. Dose response curves characterizing tyrosine kinase inhibitor sensitivity of ROS1 wild-type (WT) and mutant cell lines. Dose response cell viability assay data of Ba/F3 CD74-ROS1 WT and indicated mutant cells lines after 72-hour exposure with varying concentrations of crizotinib, entrectinib, taletrectinib, lorlatinib, repotrectinib, cabozantinib, merestinib, and gilteritinib as normalized to vehicle-treated cells. Where indicated, mean and SEM is shown from three technical replicates.

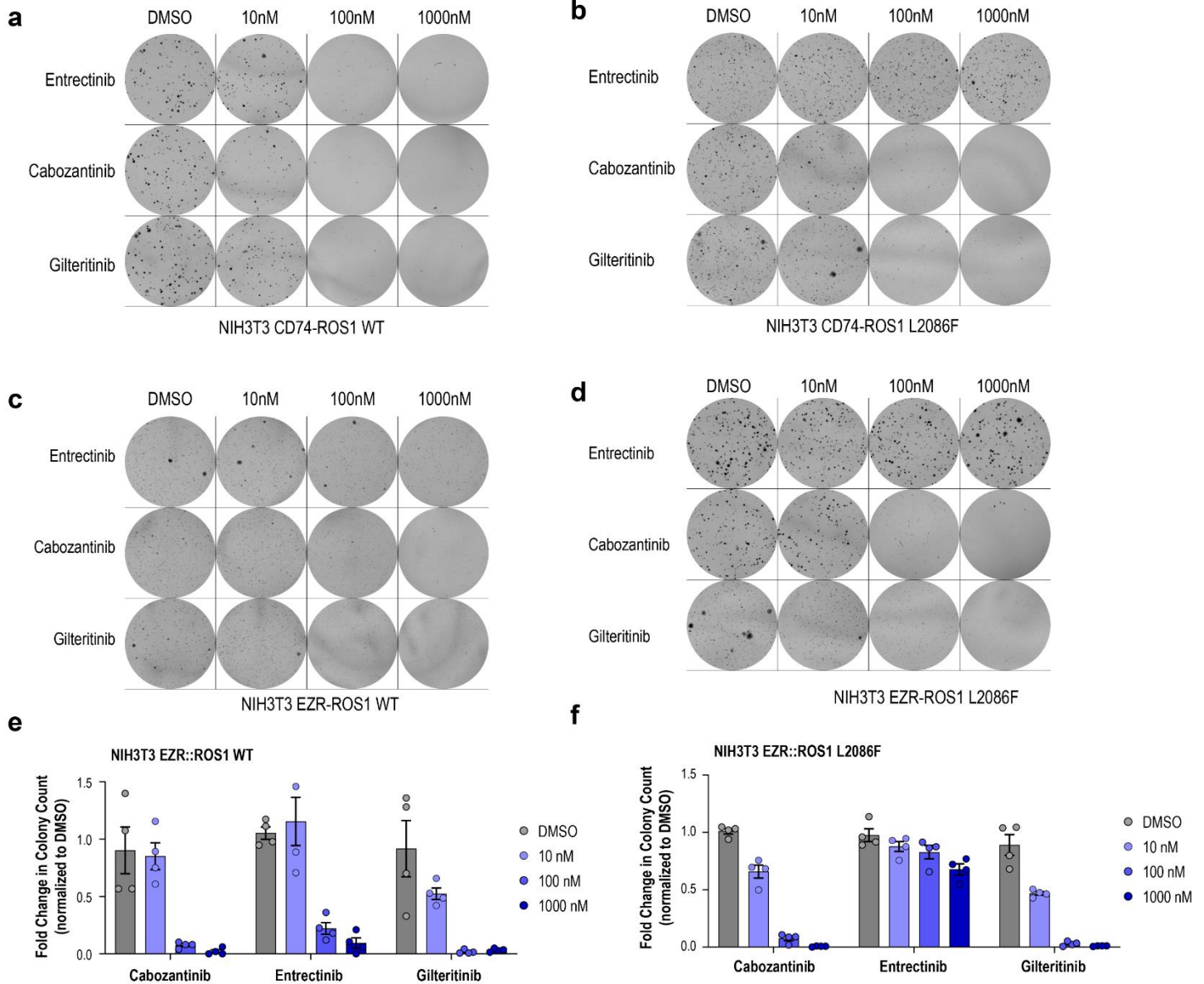
Supplementary Figure 2

Ba/F3 CD74-ROS1 mutant dose response curves



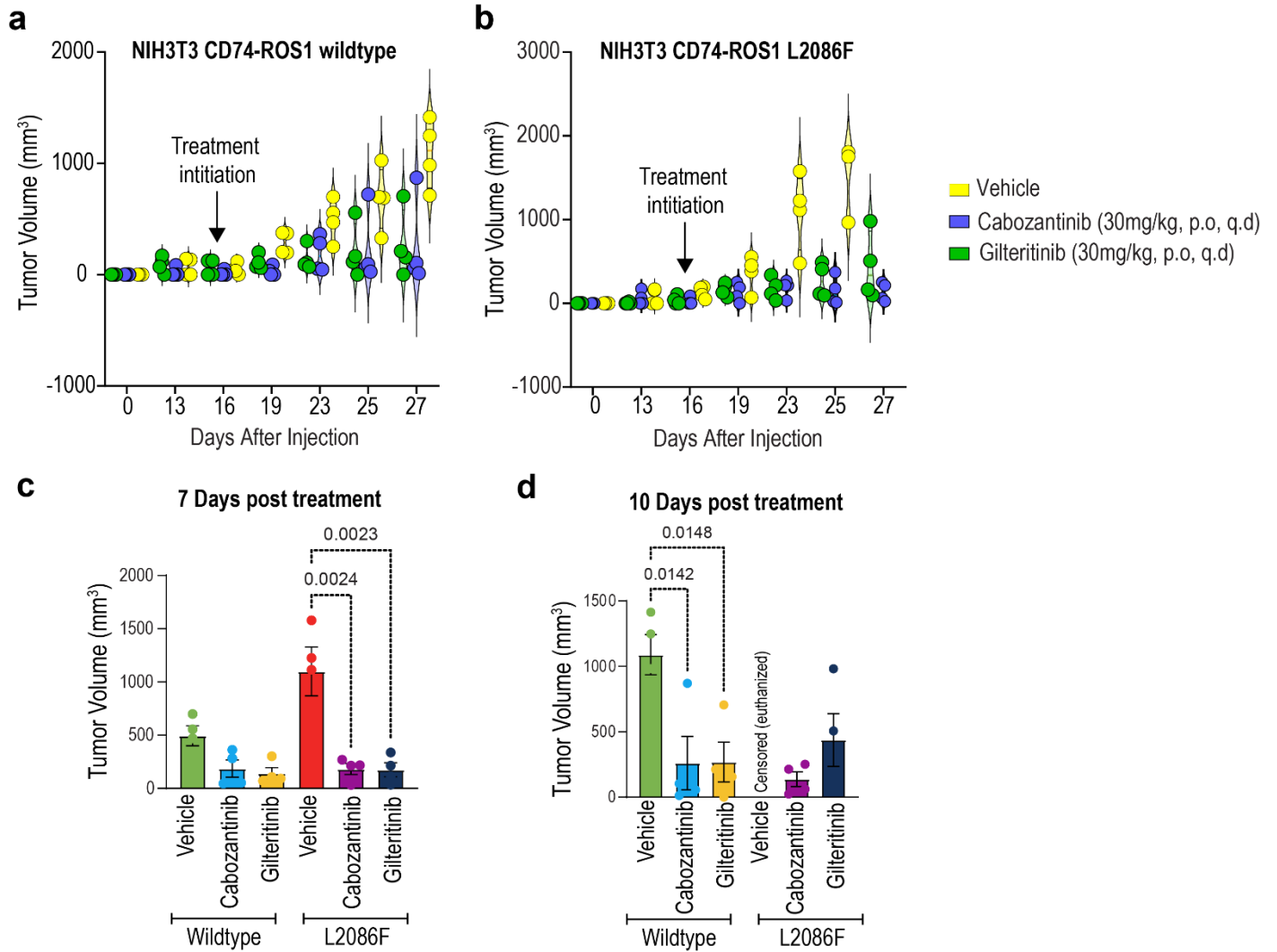
Supplementary Figure 2. Dose response cell viability assay data showing tyrosine kinase inhibitor sensitivity of ROS1 wild-type (WT), L2086F and compound mutation cell lines. Dose response cell viability assay data of Ba/F3 *CD74-ROS1* wildtype, L2086F, F2004C+L2086F and G2032R+L2086F cell lines after 72-hour exposure with varying concentrations of crizotinib, entrectinib, taletrectinib, lorlatinib, repotrectinib, cabozantinib, merestinib, and gilteritinib as normalized to vehicle-treated cells. Where indicated, mean and SEM is shown from three technical replicates.

Supplementary Figure 3



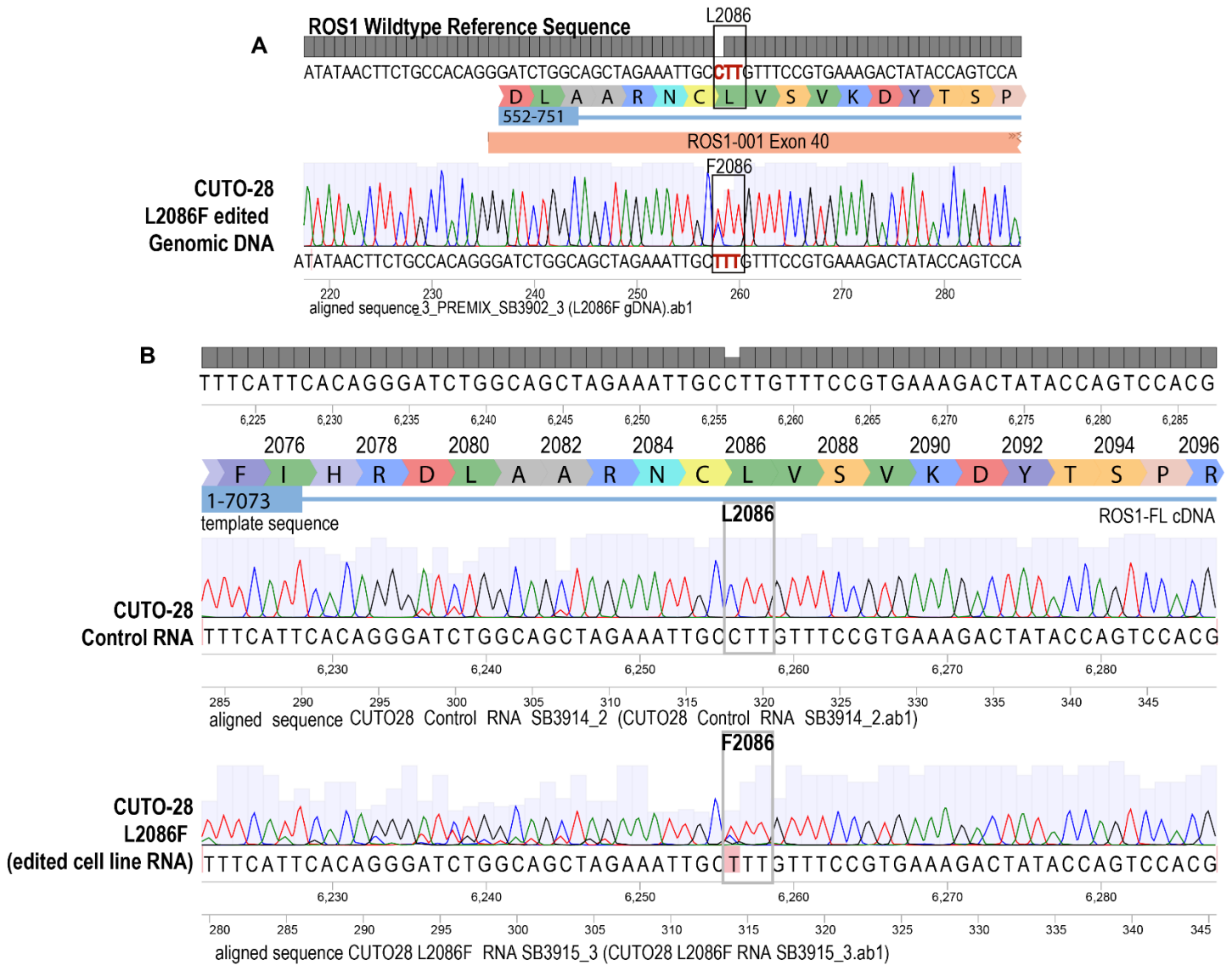
Supplementary Figure 3. Soft agar colony formation assays using NIH3T3 *EZR-ROS1* wild-type (WT) and L2086F cells. a-d. Representative images from colony formation soft agar assays using NIH3T3 CD74::ROS1 and EZR::ROS1 WT and L2086F cells in indicated concentrations of inhibitor. e-f. Colony count normalized to paired dimethyl sulfoxide (DMSO) conditions for indicated tyrosine kinase inhibitor treatment conditions from anchorage-independent soft agar assays using NIH3T3 EZR::ROS1 WT or L2086F cell lines. Data from n=4 wells per condition with mean and SEM shown.

Supplementary Figure 4



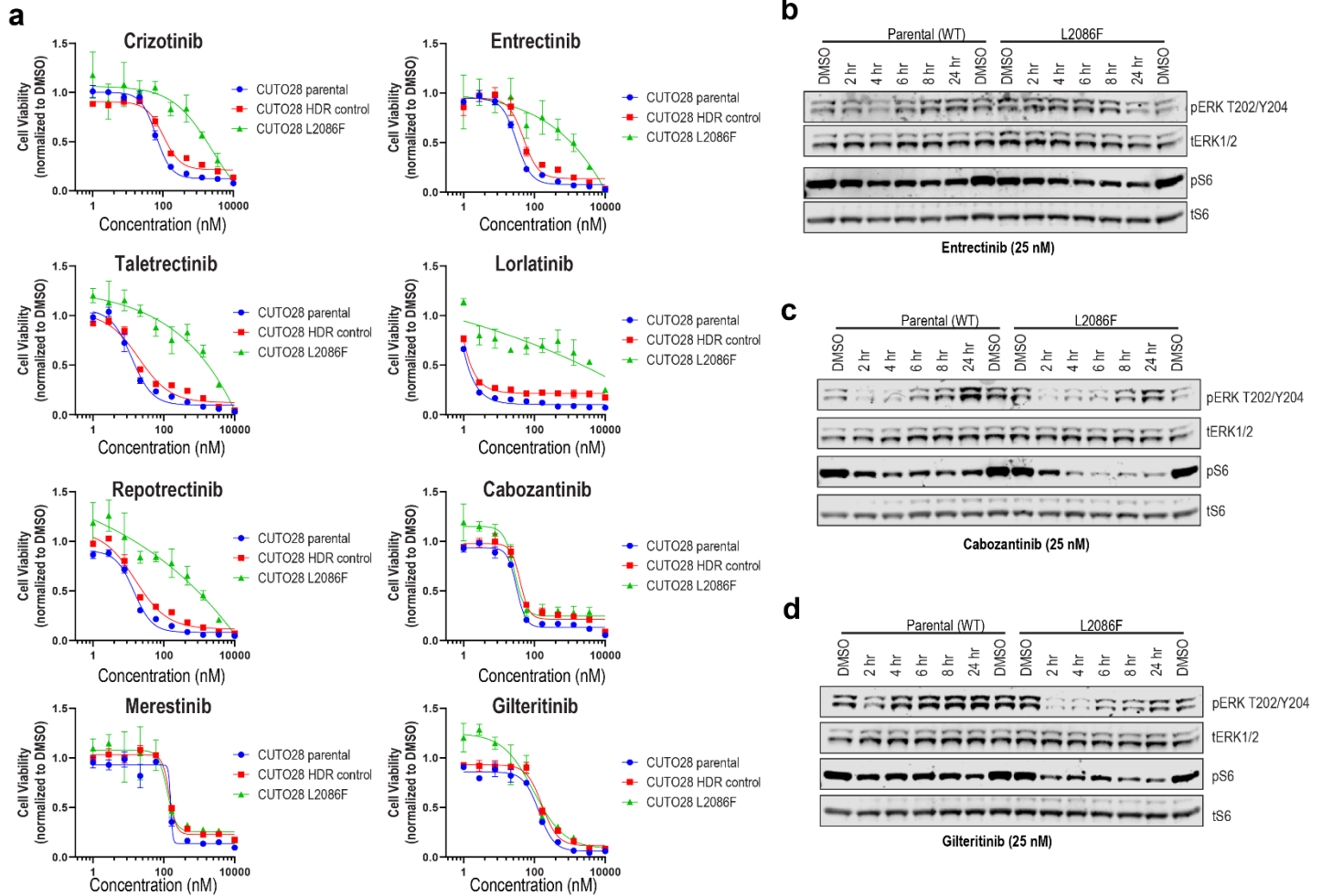
Supplementary Figure 4. In vivo antitumor efficacy of cabozantinib and gilteritinib. Time course of tumor growth of allografted NIH3T3 *CD74-ROS1* wild-type (**a**) and 2086F (**b**) subcutaneous tumors treated with cabozantinib and gilteritinib. N = 4 mice per treatment group. Arrow indicates treatment initiation. Tumor volumes at (**c**) day 7 post treatment (day 23 in experiment) and (**d**) day 10/11 post treatment (day 26/27) of treatment are shown. Mean \pm SEM are presented in the graphs. P values determined using one way ANOVA with Dunnett's multiple comparison test are shown in case of significance.

Supplementary Figure 5



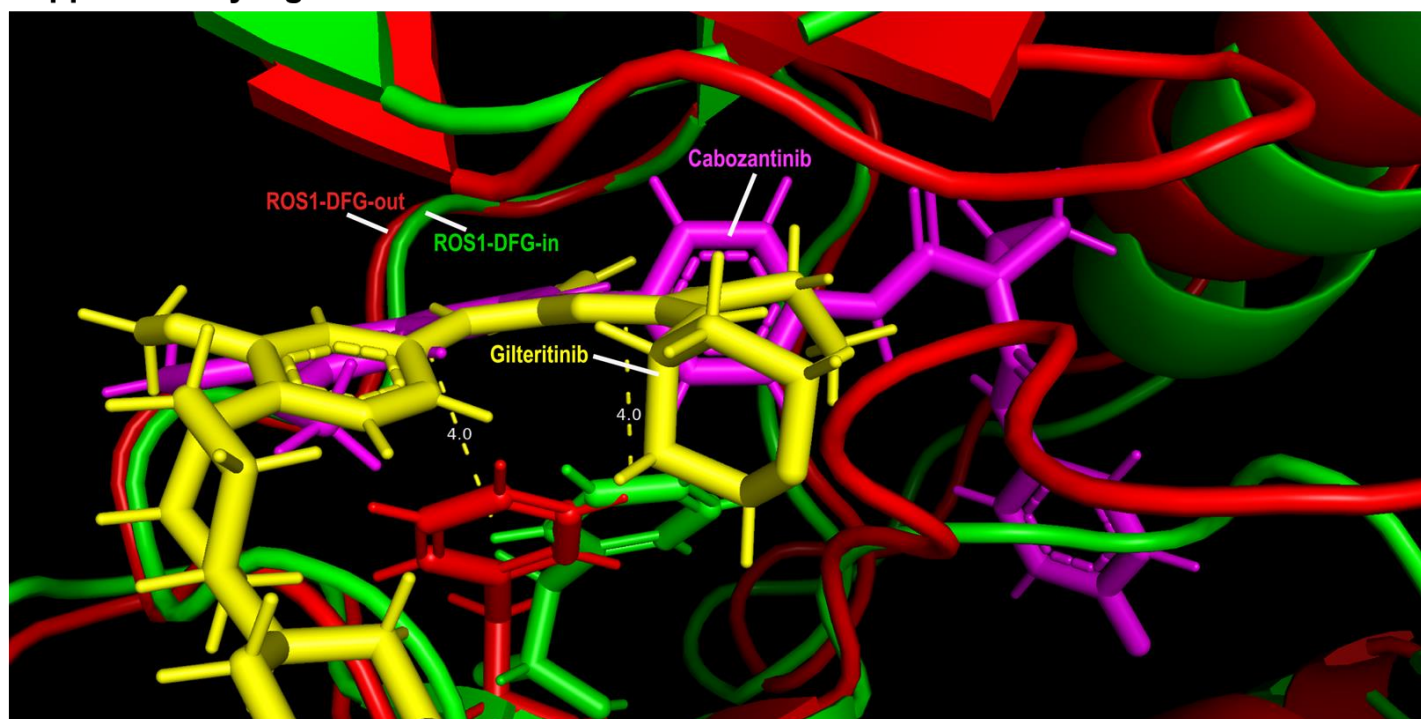
Supplementary Figure 5. Validation of genome edited endogenous L2086F mutation in the CUTO-28 L2086F cell line. Sanger sequencing on amplicons generated from CUTO-28 L2086F cell line gDNA (a) and cDNA (b) confirm the heterozygous L2086F mutation in this gene edited cell line.

Supplementary Figure 6



Supplementary Figure 6. Dose response curves characterizing tyrosine kinase inhibitor sensitivity of CUTO-28 Parental, CUTO-28 Control HDR edited and CUTO-28 L2086F mutant cell lines. a. Cell viability of indicated cells lines after 72-hour exposure with varying concentrations of crizotinib, entrectinib, taletrectinib, lorlatinib, repotrectinib, cabozantinib, merestinib, and gilteritinib as normalized to vehicle-treated cells. Where indicated, mean and SEM is shown from three technical replicates. **b-d.** Immunoblot analysis of phosphorylated and total MAPK (ERK1/2) and protein S6 from lysates generated from CUTO-28 parental and TPM3-ROS1 L2086F cells that were treated for 2, 4, 6, 8, and 24 hours with 25 nM entrectinib, cabozantinib and gilteritinib, as indicated.

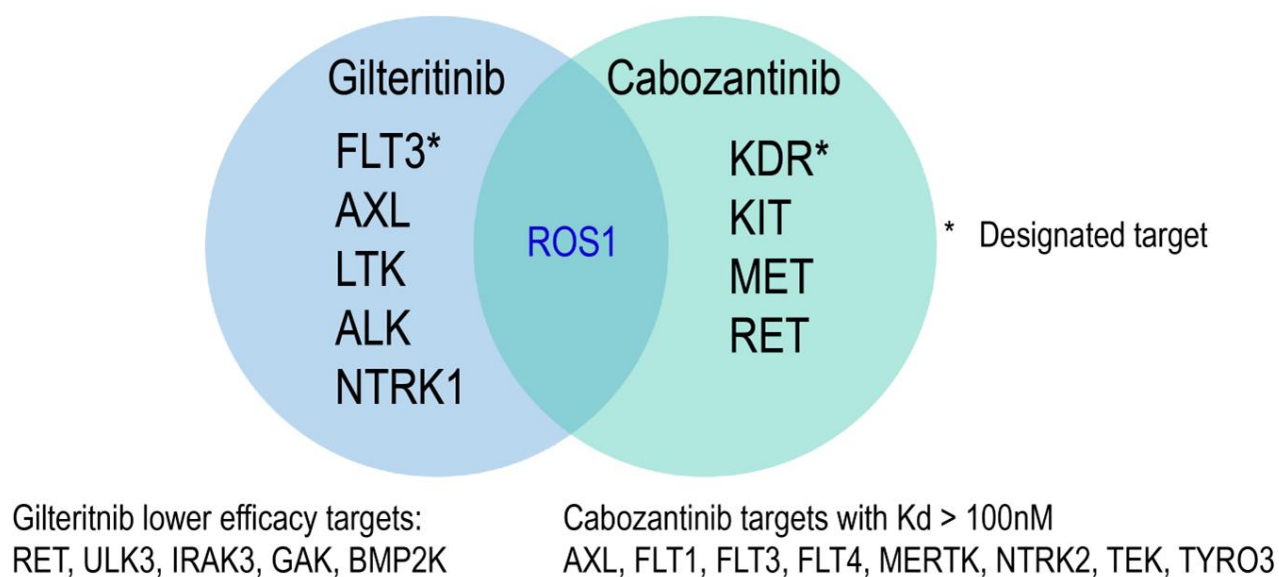
Supplementary Figure 7



Supplementary Figure 7. Distances between ROS1 L2086F and aromatic systems in predicted binding poses of cabozantinib and gilteritinib.

ROS1 DFG-in (green), gilteritinib (yellow), ROS1 DFG-out (red), cabozantinib (purple), measurements are shown from the center of the phenyl group of ROS1 L2086F and the pyrazinamide moiety of gilteritinib and the quinoline moiety of cabozantinib.

Supplementary Figure 8

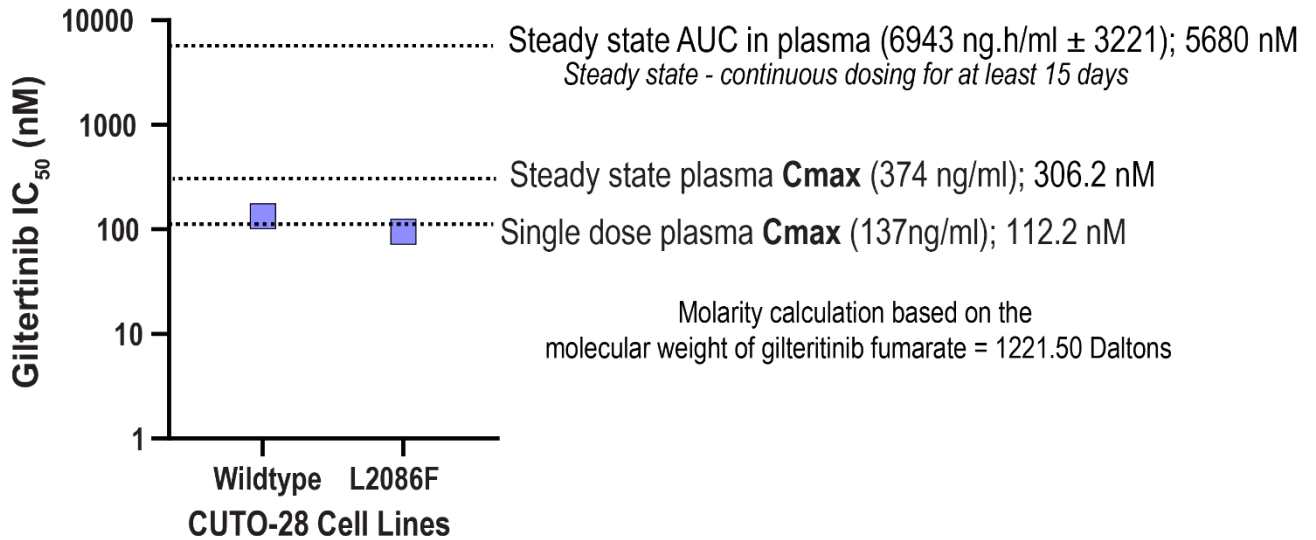


Supplementary Figure 8. Spectrum of kinase inhibition by gilteritinib and cabozantinib.

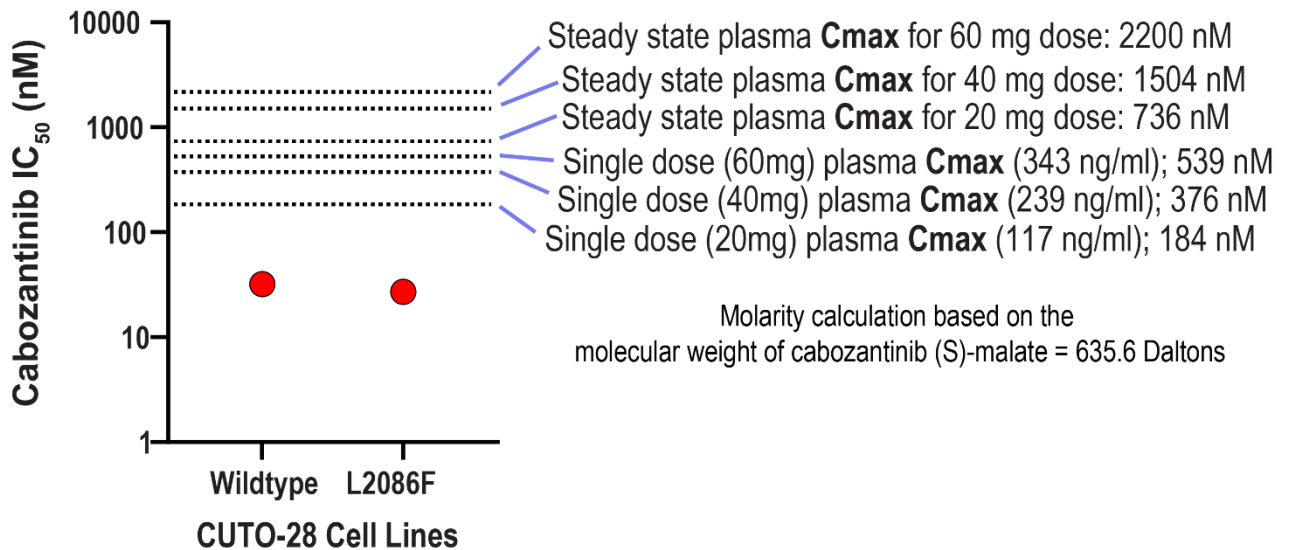
The respective kinase inhibition profiles were examined using the Harvard Medical School's Library of Integrated Network-based Cellular Signatures (LINCS) Small Molecule profiling database (<https://lincs.hms.harvard.edu/db/sm/10194-106/>) for cabozantinib, and data from the publication by Klaeger et al.³⁸ for gilteritinib's inhibition profile.

Supplementary Figure 9

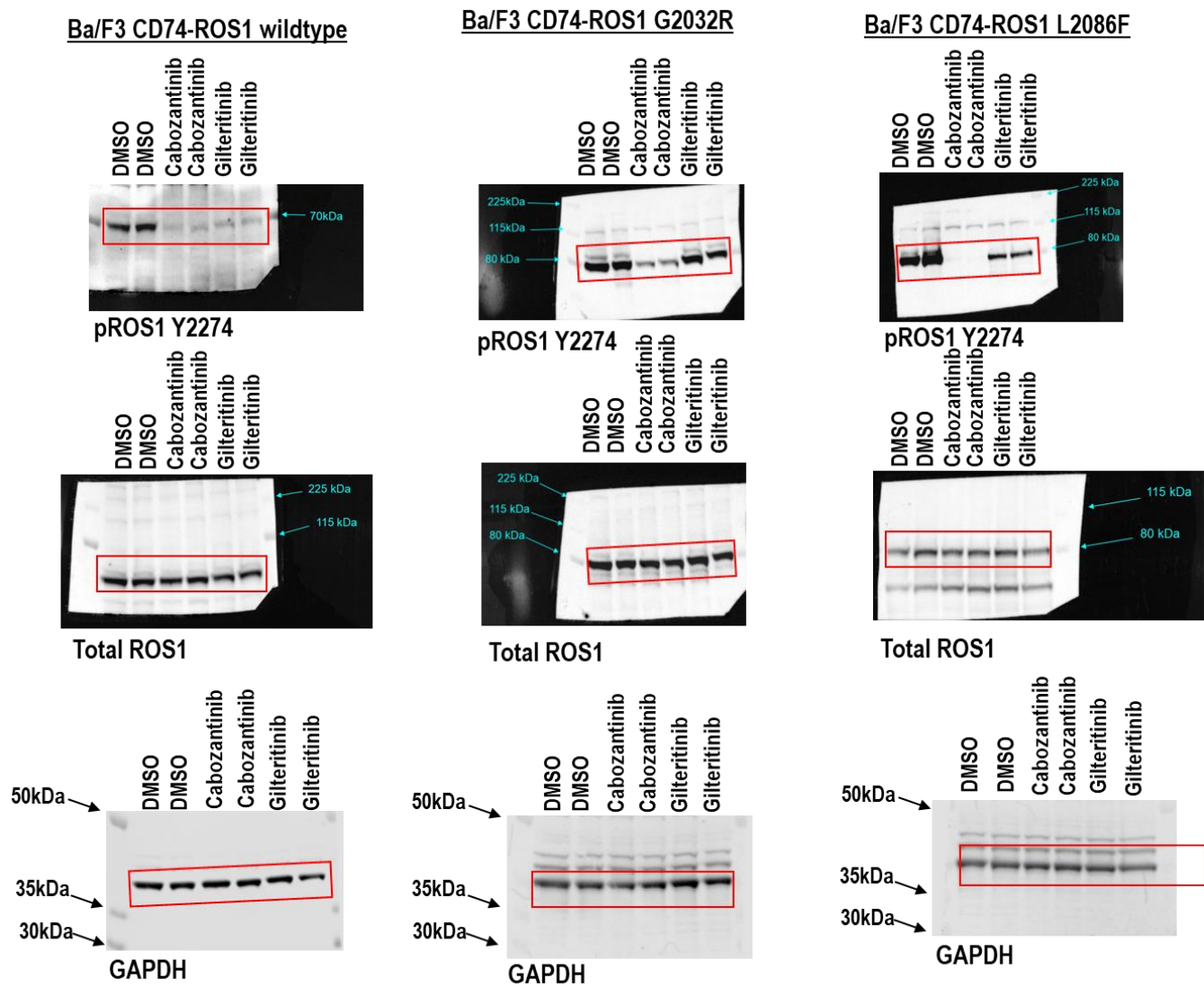
- a** Gilteritinib PK data from human studies relative to cell based IC_{50} with CUTO-28 cells
Data from FDA recommended human gilteritinib dose - 120mg/PO/QD



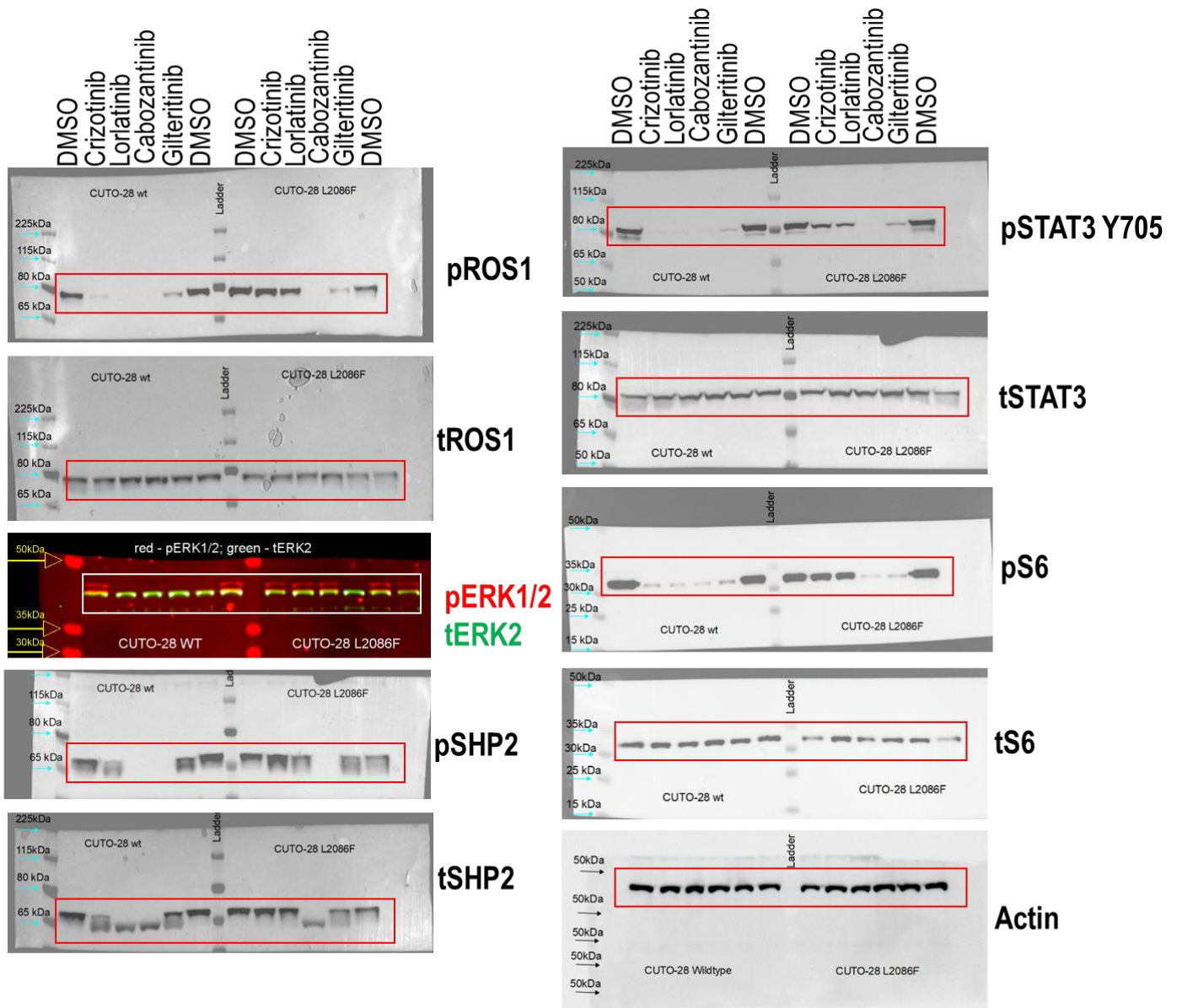
- b** Cabozantinib PK data from human studies relative to cell based IC_{50} with CUTO-28 cells
Data from FDA recommended human cabozantinib dose - 60 mg/PO/QD compared to 40 and 20 mg.



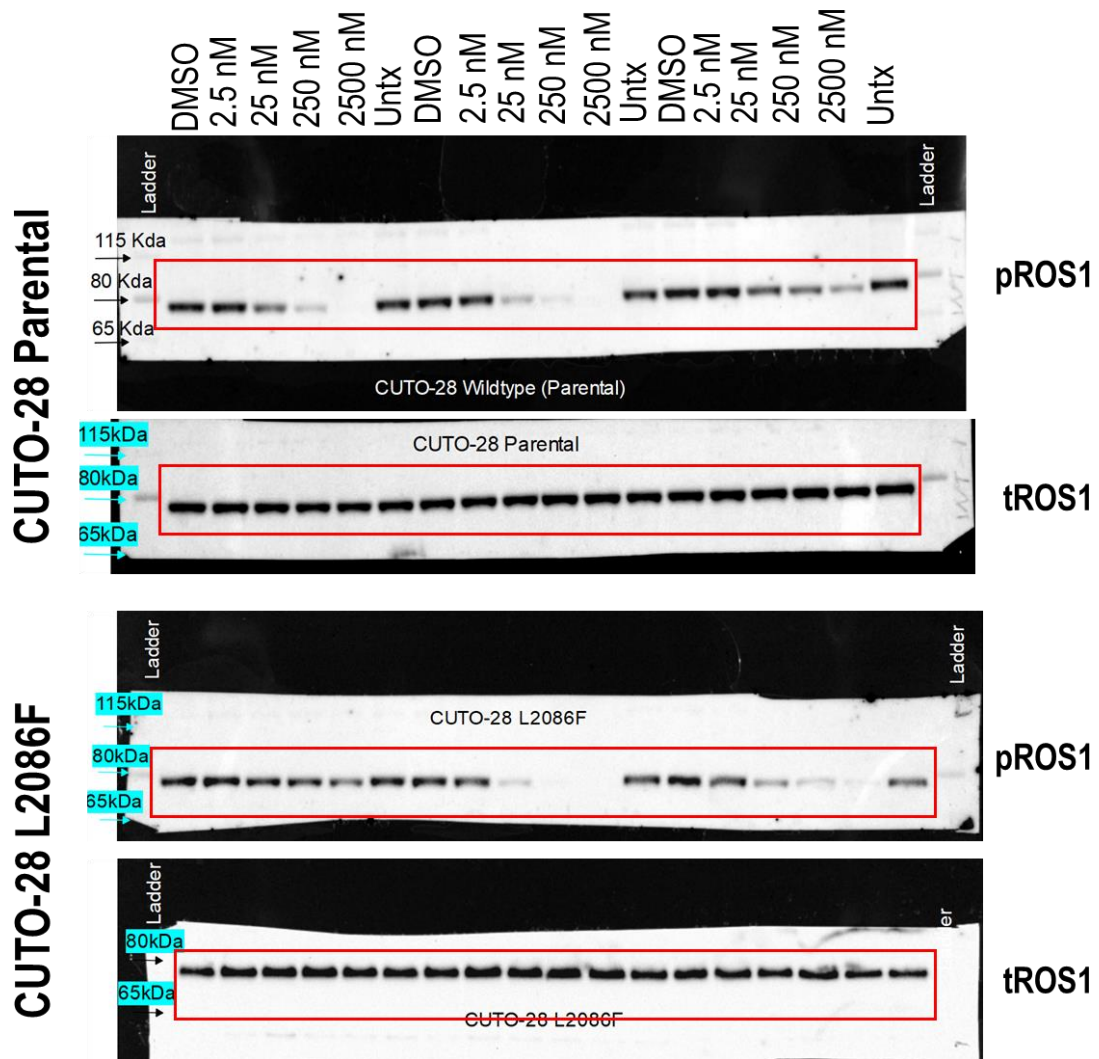
Supplementary Figure 9. Pharmacokinetic (PK) profiles of gilteritinib and cabozantinib juxtaposed with cell-based IC_{50} for CUTO-28 wildtype and L2086F mutant cells. **a.** Gilteritinib (Xospata™) PK profile was determined from FDA prescribing information insert (https://www.accessdata.fda.gov/drugsatfda_docs/label/2019/211349s001lbl.pdf), **b.** cabozantinib PK data were from publication by Ngyuyen et al³². In both cases the concentrations in molarity units are calculated based on clinically reported ng/ml unit PK data and molecular weights of respective human formulated drugs.



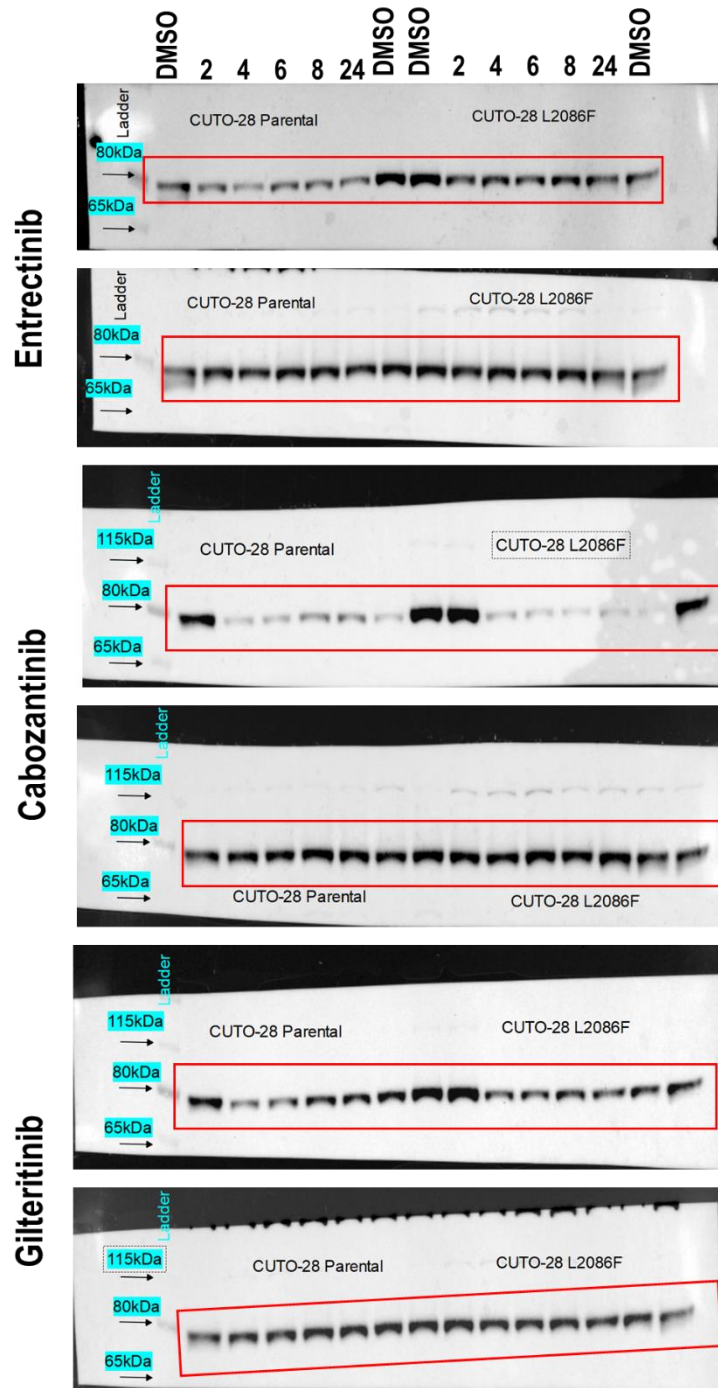
Supplementary Figure 10a. a. Uncropped western blot chemiluminescent images from TKI-treated treated Ba/F3 cell lysate blotting shown in Figure 1c. Note: The images shown below are merged composites of the chemiluminescent image and the colorimetric membrane image. These are shown as composites to clearly delineate the outline of the blot and depict protein ladders. When imaging the GAPDH blot, the colorimetric image was not saved. ROS1 antibody blots were developed using chemiluminescent substrate. GAPDH blots were developed using LICOR imager.



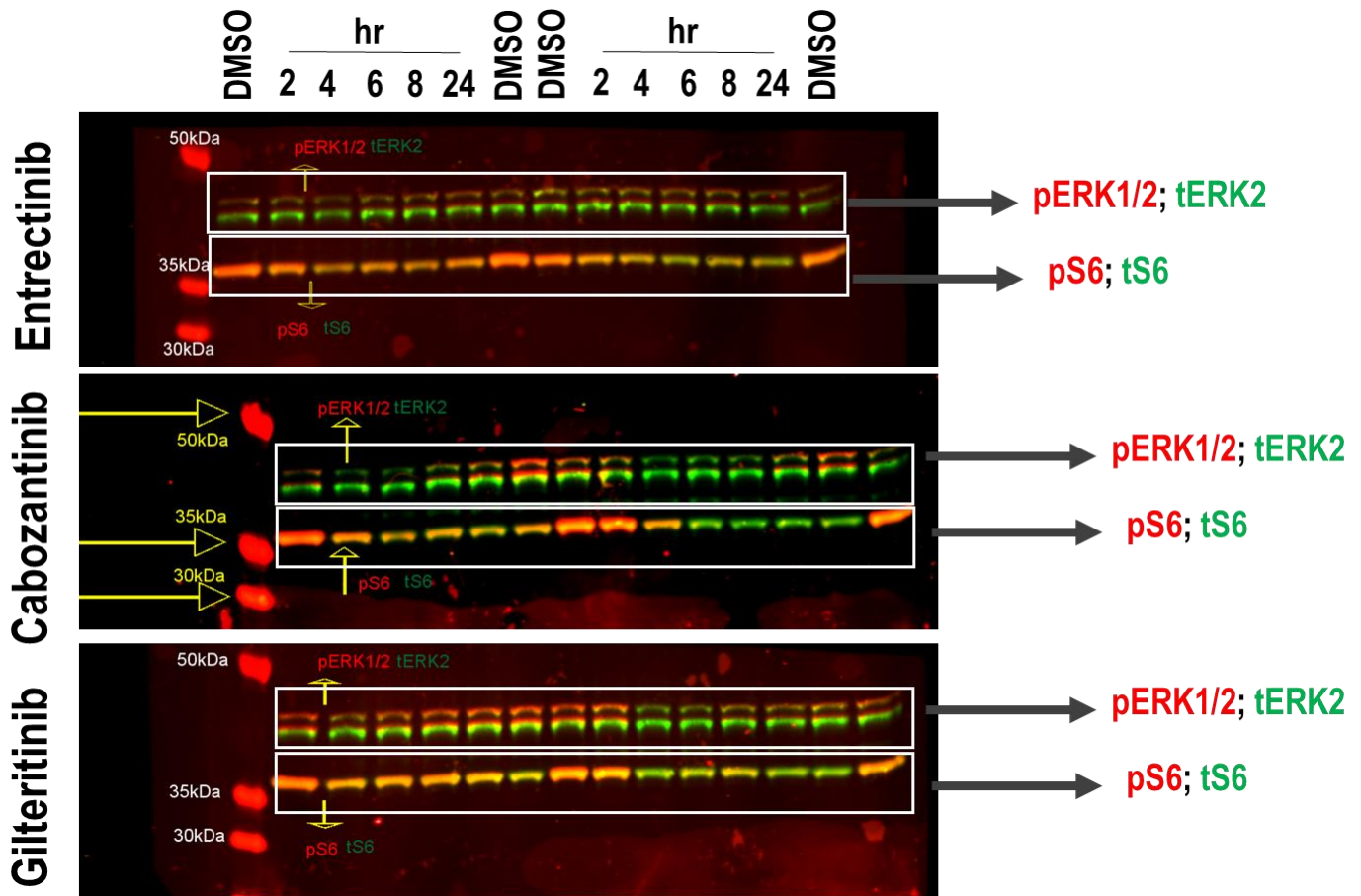
Supplementary Figure 10b. Uncropped western blot chemiluminescent images from TKI-treated CUTO-28 Parental and CUTO-28 L2086F cell lysate blotting in Figure 2c. The images shown below are merged composites of the chemiluminescent image and the colorimetric membrane image. These are shown as composites to clearly delineate the outline of the blot and depict protein ladders. Except of phospho-ERK1/2 and total ERK2, all blots were developed using chemiluminescent substrate. ERK signaling (phospho-ERK1/2 and total ERK2) were multiplexed via detection with Anti-Rabbit-Alexa680 and Anti-Mouse-Alexa790 secondary antibodies. Figure 2 shows black and white converted images. Composite red/green image from LI-COR imaging is shown below.



Supplementary Figure 10c. Uncropped western blot from chemiluminescent images TKI-treated CUTO-28 Parental and CUTO-28 L2086F cell lysate blotting in Figure 2d. The images shown below are merged composites of the chemiluminescent image and the colorimetric membrane image. These are shown as composites to clearly delineate the outline of the blot and depict protein ladders.



Supplementary Figure 10d. Uncropped western blot chemiluminescent images from TKI-treated CUTO-28 Parental and CUTO-28 L2086F cell lysate blotting in Figure 2e. The images shown below are merged composites of the chemiluminescent image and the colorimetric membrane image. These are shown as composites to clearly delineate the outline of the blot and depict protein ladders.



Supplementary Figure 10e. Uncropped western blot chemiluminescent images TKI-treated CUTO-28 Parental and CUTO-28 L2086F cell lysate blotting in Supplementary Figure 6. ERK and S6 signaling (phospho-ERK1/2 and total ERK2, phospho-S6 and total S6) were multiplexed via detection with Anti-Rabbit-Alexa680 and Anti-Mouse-Alexa790 secondary antibodies. Figure S6 shows the original black and white images from each respective channel separately. Composite red/green images from LI-COR imaging are shown below.

Supplementary Table 1. Adverse events associated with cabozantinib, gilteritinib in the CELESTIAL and ADMIRAL clinical trials. Heat map depicts a visual summary of the incidence of grade 3 or greater adverse events for cabozantinib and gilteritinib.

	ADVERSE EVENTS OCCURRING IN \geq20% OF PATIENTS	INCIDENCE OF GRADE \geq3 ADVERSE EVENTS (%)
CABOZANTINIB 60 MG CELESTIAL CLINICAL TRIAL	Diarrhea	10
	Decreased appetite	6
	Palmar-plantar erythrodysesthesia	17
	Fatigue	10
	Nausea	2
	Hypertension	16
	Vomiting	<1
	Increased in aspartate aminotransferase level	11
	Asthenia	7
	Febrile neutropenia	46
	Anemia	47
	Pyrexia	3
	Increase in alanine aminotransferase level	14
	GILTERITINIB 120 MG ADMIRAL CLINICAL TRIAL	Diarrhea
Increased in aspartate aminotransferase level		15
Hypokalemia		13
Constipation		1
Platelet count decreased		<1
Fatigue		2.4
Cough		<1
Thrombocytopenia		23
Headache		1
Peripheral edema		<1
Vomiting		<1
Dyspnea		4
Blood alkaline phosphatase increased		3
CRIZOTINIB 250 MG BID NCT00932893		Nausea
	Vomiting	1
	Constipation	2
	Increase in aminotransferase	16
	Fatigue	2
	Dizziness	1

Supplementary Table 1. (Contd.)

Incidence of Grade \geq 3 Adverse Events (% indicated in heat map cell)

	Cabozantinib	Gilteritinib	Crizotinib
Palmar plantar erythrodysesthesia	17	0	0
Hypertension	16	0	0
Increased in AST/ALT	11	15	16
Diarrhea	10	4	0
Fatigue	10	2	2
Asthenia	7	0	0
Decreased appetite	6	0	0
Nausea	2	0	1
Constipation	1	1	0
Vomiting	1	1	1
Febrile Neutropenia	0	46	0
Anemia	0	47	0
Hypokalemia	0	13	0
Thrombocytopenia	0	23	0
Headache	0	1	0
Peripheral edema	0	1	0
Dyspnea	0	4	0
Blood AlkPhos increased	0	3	0
Dizziness	0	0	1

Unique Adverse Events Summary

Cabozantinib: Decreased appetite, palmar-plantar erythrodysesthesia, hypertension, and asthenia.

Gilteritinib: Febrile neutropenia, anemia, and thrombocytopenia.

Crizotinib: Dizziness

Supplementary Table 2. Primer sequences used to support polymerase chain reaction, site directed mutagenesis and CRISPR/Cas9 genome editing experiments.

Primer Name	Primer Sequence (all indicated 5' - 3')
ROS1 F2004C S	GGCACATCTGATGAGCAAATGTAATCATCCCAACATTCTG
ROS1 F2004C AS	CAGAATGTTGGGATGATTACATTTGCTCATCAGATGTGCC
ROS1 L2026M F	CCTCCATCAGTTCCATGATAATGTATTGGGGTTCATTCA
ROS1 L2026M R	TGAATGAACCCCAATACATTATCATGGAAGTATGGAAGG
ROS1 G2032R AS	AATAAGTAAGAAGGTCTCTCCCTCCATCAGTTCCAG
ROS1 G2032R S	CTGGAAGTATGAGAGGAGACCTTCTTACTTATT
L2086F_REV	AGTCTTTCACGGAAACAAAGCAATTTCTAGCTGCCAG
L2086F_FWD	CTGGCAGCTAGAAATTGCTTTGTTCCGTGAAAGACT
L2086FguideF	caccgTATAGTCTTTCACGGAAACA
L2086FguideR	aaacTGTTTCCGTGAAAGACTATAc
L2086seqF	taatgcaggcagggcttaa
L2086seqR	tgctgagaccaggaatagta
ROS1 F10	AGAAGGGTCCACAGACCAG
ROS1 R13	TCCAGTCTCCCTCCTGTTTG
L2086F HDR template	ATTTCTGGAAGTtattgtgttattattattattattaAATATAACTTCTGCCA CAGGGATCTGGCAGCTAGAAATTGctTTGTTTCCGTGAAAGACTAT ACCAGTCCACGGATAGTGAAGATTGGAGACTTTGGACTCGCCAGA GACATCTATAAAAATGA